USING ^{10}Be TO CONSTRAIN EROSION RATES OF BEDROCK OUTCROPS, GLOBALLY AND IN THE APPALACHIAN MOUNTIANS

A Thesis Progress Report Presented

by

Eric W. Portenga

to

The Faculty of the Geology Department

of

The University of Vermont

November 19, 2009

Accepted by the Faculty of the Geology Department, the University of Vermont, in partial fulfillment of the requirements for the degree of Masters of Science specializing in Geology.

The following members of the Thesis Committee have read and approved this document before it was circulated to the faculty.

_____
Paul Bierman (Adviser)

_____
Donna Rizzo

_____
Laura Webb

_____

Date Accepted: _____

1.0 Introduction

Rock outcrops are features of landscapes around the world; however, little is known about how quickly these landforms erode through time. Exposed bedrock erosion rates are difficult to constrain because they are so slow (Saunders and Young, 1983). The advancement of accelerator mass spectrometry has allowed cosmogenic nuclides, such as ^{10}Be, to be used as indicators of erosion rates on bedrock landforms on the 10^3-10^6 year timescale (Lal, 1991).

The study of exposed rock is often overlooked in the literature and only a few studies have focused solely on exposed bedrock erosion rates (Bierman and Caffee, 2002; 2001; Cockburn et al., 2000; Hancock and Kirwan, 2007). Studies tend to focus on the understanding how rock weathers under a mantle of soil or boulders (Granger et al., 2001; Heimsath et al., 1997) and at the scale of fluvial systems (Brown et al., 1995; Clapp et al., 2000; von Blanckenburg et al., 2004). It is important to understand the erosion rate of bedrock because in many locations it sets the pace of landscape change.

My research will add to the select few studies whose sole focus is exposed bedrock erosion by measuring erosion rates on bedrock exposures in the central Appalachian Mountains. To place my data in a broader context, I have created a global ^{10}Be exposed bedrock erosion rate database. I will compare erosion rates from the Appalachian Mountains to those found in other settings around the world. I will compare the erosion rates I measure in the Appalachian Mountains to those determined by the basin-averaged ^{10}Be technique. It is important to summarize and analyze the current literature in order to create a context through which new bedrock erosion data can be compared, therefore becoming more meaningful to those who study current landscape evolution as well as those who study how rocky landforms have changed through time in the past.

2.0 Work Completed

2.1 Exposed Bedrock Erosion Rate Summary

Erosion rates modeled from *in situ* [10]Be concentrations have been compiled from published and non-published sources and placed into a global dataset (Fig. 1). Erosion rates were recalculated from the original [10]Be concentrations using a consistent production rate of [10]Be. The data have been summarized and analyzed statistically to compare the erosion rate of exposed rock with environmental parameters; latitude, elevation, local relief (r=5km), mean annual precipitation, mean annual temperature, seismicity (peak ground acceleration), climate zone, seismic zone, and lithology are the parameters which I have deemed important for this summary. In order to minimize errors introduced to the analyses by multiple sources of individual parameters utilized in each publication, the most up-to-date global datasets for each of these parameters were used (Table 1).

2.2 Field Work

Two weeks were spent in the field collecting rock samples from exposed bedrock outcrops along the crests of ridgelines and spur ridges in the central Appalachian Mountains (VA, WV, MD, and PA). The field site was selected to be within the Potomac and Susquehanna River basins in order to compare bedrock erosion rates with basin-averaged erosion rates previously and presently being analyzed by other graduate students (Duxbury, 2009; Reuter, 2005; Trodick, In Progress). Furthermore, all samples are from unglaciated ridges outside the glacial margin in order to be consistent with previous sampling strategies employed by students using basin-averaged [10]Be methods.

A total of 74 samples were collected from 27 different locations within the two river basins ($n_{Potomac}$=48; $n_{Susquehanna}$=26; Fig. 2). Time in the field was limited; therefore, prior knowledge of where rock actually crops out of the landscape was necessary. Site locations were previously determined using ArcGIS (vers. 9.3) by finding quartz-rich lithologies within National and State Park and Forest boundaries, easily accessible by either road or hiking trail.

At least two samples were collected at each specific location to calculate an erosion rate variance at each site. At some sites, more than one rock outcrop was available, in which case three or four samples were taken. This will allow not only allow variance in single outcrop erosion rates to be calculated, but also variance at the local level. In some cases, where more than one outcrop was present near or on a cliff, more than two samples were collected in order to determine variance between erosion rates near a sharp change in elevation and rates of rock set back from a drop-off.

2.3 Lab Work

Rock samples collected in the field were brought back to the Cosmogenic Nuclide Laboratory at the University of Vermont for quartz purification. Samples were crushed and ground before being sieved into 0-250µm, 250-850µm, and 850+µm grain-size fractions. The 250-850µm size fraction was magnetically separated to remove magnetic mineral phases.

The non-magnetic size fraction of each sample was then etched in a dual 6N HCl solution for a total of 48 hours followed by three etches in a 1% HF/HNO$_3$ solution for a total of 72 hours. Acid etches remove non-quartz mineral phases and other contaminants on the outside of quartz grains. Following the first round of acid etches, samples were examined under a microscope for quartz purity, and if sizable amounts of minerals other than quartz remained, the

minerals were separated by heavy-liquid density separation. To complete cleaning, all samples were then etched in a 0.5% HF/HNO$_3$ solution for a total of ten days.

Before each sample can be tested for [10]Be content, the quartz purity must be tested. A 0.250g aliquot from each sample was digested in an HF/H$_2$SO$_4$ solution. The HF evaporated overnight leaving behind the digested sample in a small bead of H$_2$SO$_4$, to which deionized water was added, creating a 1% H$_2$SO$_4$ solution which was tested for cation concentrations using inductively coupled plasma optical emission spectrometry.

3.0 Initial Results

3.1 Statistical Analyses of Exposed Bedrock Erosion from the Global Compilation

Concentrations of [10]Be vary with latitude because the [10]Be production rate is dependent on the influx of cosmic rays which are more strongly attenuated at the equator by Earth's magnetic field and less so at high latitudes; production rates also vary with elevation because cosmic rays attenuate as they travel through the atmosphere (Lal, 1991). All measured [10]Be concentrations are corrected for these variations and normalized to sea level at high latitudes (>60°).

Erosion rates vary by latitude; because latitude and climate co-vary, the observed relationship between latitude and erosion rate may well be driven by climate (Figs. 3, 4). The latitude/erosion rate plot shows a gap between 50° - 70° north and south signifying the location of the Southern Ocean, where no rock is exposed, and the northern latitudes where glacial activity complicates the interpretation of [10]Be concentrations as erosion rates. While elevation yields the weakest fit of all variables analyzed (R^2=0.001; p=0.6176; Fig. 5), local relief within a 5km radius of the sample site yields the overall best fit (R^2=0.150; p<0.0001; Fig. 6).

Peak ground acceleration (Fig. 7) is used as a proxy for seismic activity and is defined as a magnitude of ground motion with a 10% chance of being exceeded within 50 years (Giardini et al., 1999). Although basin-average erosion rates around the world correlate well with seismicity (Reuter, 2005), point specific erosion rates do not display as strong of a relationship (R^2=0.021; p=0.007; Fig. 8). [10]Be data has been collected for basin-averaged erosion rates in regions of extremely high tectonic activity – in the Himalayas, for example (Vance et al., 2003) – whereas extremely few studies include bedrock erosion rates for areas of high tectonic activity (Ivy-Ochs et al., 2007; Kober et al., 2007). As seismic intensity increases, erosion rates also increase (Fig. 8). We also observe that exposed bedrock in seismically active areas (n=69; 19.6±3.0 m My^{-1}; Fig. 9), determined by their seismicity in the Global Seismic Hazard Map by Giardini et al. (1999), erodes significantly faster than that in inactive areas (p<0.0001; n=309; 8.4±1.2 m My^{-1}).

The specific lithology of each sample was provided in its respective publication; however, the specific lithology was simplified in the broadest sense possible into sedimentary, igneous, and metamorphic rocks in order to maintain robust sample populations. Five samples came from quartz veins, and since these were the only monomineralic samples in the compilation, they were put into their own lithologic category. Erosion rates should vary with lithology as sedimentary and metamorphic rocks have inherent weaknesses along bedding and foliation planes whereas igneous rocks and pure quartz are composed of interlocking mineral crystals. This is reflected in the global data as sedimentary and metamorphic rocks have statistically similar erosion rates (n=66, 18.5±2.8 m My^{-1} and n=52, 12.9±1.9 m My^{-1}, respectively; Fig. 10); furthermore, sedimentary rocks erode significantly faster than igneous rocks (n=255, 8.0±1.2 m My^{-1}) and quartz (n=5, 2.2±0.3 m My^{-1}) whereas metamorphic rocks

only erode significantly faster than igneous rocks (Fig. 10). Within each lithology, samples in seismically active zones erode faster than those in seismically inactive zones.

Bedrock studies have often tried finding a direct link between erosion rate and climate (Bierman and Caffee, 2002; 2001). An updated version of the Köppen-Geiger climate classification system (Peel et al., 2007) combines temperature and precipitation data and utilizes five main climate regions: tropical, arid, temperate, cold, and polar (Fig. 11). Using that classification scheme, we see that exposed rock in temperate climates erode significantly faster than those in any other climate zone ($n=78$; 25.5 ± 3.7 m My^{-1}; Fig. 12). Erosion rates in cold climates ($n=32$; 15.8 ± 2.4 m My^{-1}) are significantly higher than those in tropical, arid, and polar climates ($n=14$, 5.3 ± 0.8 m My^{-1}; $n=277$, 5.9 ± 0.9 m My^{-1}; and $n=27$, 1.2 ± 0.2 m My^{-1}; Fig. 12). It is important to note that sample populations for climate zones vary.

Mean annual precipitation shows the second strongest correlation with erosion rates on the global scale ($R^2=0.133$; $p<0.0001$; Figs. 13, 14). Erosion rates are generally higher in areas with high rainfall as well as those where temperatures allow moisture to remain in contact with exposed rock (i.e. tropical, temperate, and cold climate zones), facilitating processes such as freeze-thaw cycling and chemical weathering. The relationship between erosion rates and mean annual temperature is more complicated (Figs. 15, 16); however we can see that temperate climates, where processes like freeze-thaw cycling are prevalent, there is a sharp peak in erosion rates. As temperature reaches extremely high and low levels, erosion rates are at their lowest.

Forward stepwise regressions were produced for categorical data (i.e. lithology, climate zone, and seismic activity). The regression ranks each input variable by the p-value generated by an F-test. If the p-value is less than the Probability to Enter, the variable is entered into the multiple regression analysis. Variables are entered into the analysis one at a time. Once a

variable is entered into the analysis, a new *p*-value is assigned to the variable based on how much it improves the multivariate regression. If the new *p*-value is less than the Probability to Leave, the variable remains in the test; however, if it is greater than the Probability to Leave, the variable is removed. This step-by-step analysis considers all variables but only fits a regression through those that are statistically important (Fig. 17).

This multivariate regression shows that, on a global scale, exposed rock outcrops erode very slowly ($n=378$; 10.4 ± 1.6 m My^{-1}) and that combinations of presented variables only describe 27.9% of the variability seen in erosion rates. On the global scale, the mean annual temperature is the only significantly unimportant variable considered. Unexplained variability in erosion rates generally decreases as soon as categorical stratification of the data is applied to the regression. The multivariate regression also shows that of individual variables, mean annual precipitation, latitude, and local relief provides the strongest correlations with erosion rates both at a global and stratified scales.

3.2 Biases Inherent to the Data

This summary of erosion rates and subsequent analyses is not without biases or caveats. The samples come from all over the globe; yet, there are large portions of land that have yet to be sampled (Fig. 1). Some of this sampling bias comes from the fact that large portions of Earth have been glaciated which limits the interpretative power of ^{10}Be concentration measurements in regards to erosion rates. The majority of the data come from outcrops in easily accessible regions of the world; many unsampled locations are subject to political unrest and weak economies. The data also come solely from quartz-bearing lithologies and this limits the distribution of potential sampling sites.

Some climate zones and lithologies are undersampled which could lead to misinterpretation of the data. For example, rainfall is high in the tropics and has a high potential to erode rock, yet erosion rates in these regions are not any higher than those in polar and arid climates where precipitation is scarce. There is a chance the average erosion rate in the tropics would increase if more samples were collected than the 14 currently in the database.

Pertinent structural information such as joint spacing and fracture density for each site are rarely provided. These are important clues as to how easily pieces of rock on the surface of the outcrops might be removed, thus affecting the ^{10}Be concentration used to make erosion rate interpretations.

4.0 Work to Complete

4.1 Global Summary Publication

I presented the results of the global erosion rate summary at the GSA Annual Meeting in Portland, Oregon and received suggestions about a few more sets of bedrock erosion data to include in the summary. Once the bedrock data is completely updated, I will also update the basin-averaged global dataset compiled by Joann Reuter in 2005 so the two methods can be compared on the global scale. The synthesis of these two global summaries will be the basis of my first publication.

4.2 Continued Appalachian Sample Laboratory Work

Seventy-two samples collected in the field have had quartz purity tests (two samples were deemed unsuitable for the project and discarded). The output data from the ICP-OES has been scrutinized, and it has been determined that ten samples are not clean enough to be brought into

the *In Situ* Laboratory for final AMS preparation. These ten samples will return to the mineral separation laboratory for one week-long etch in 0.5% HF/HNO_3 and be retested for quartz purity. Once all samples pass purity tests, only 66 will make it to the AMS run at Lawrence Livermore National Laboratory – 6 samples will need to be culled. Once in the *In Situ* Laboratory, samples will be digested and run through cation and anion exchange columns to separate ion species in solution. The Be fraction will be saved, packaged, and brought to Lawrence Livermore to be tested using AMS.

5.0 Timeline

A detailed timeline for the completion of my thesis is available in Table 2.

6.0 References

Belton, D.X., Brown, R.W., Kohn, B.P., Fink, D., and Farley, K.A., 2004, Quantitative resolution of the debate over antiquity of the central Australian landscape: implications for the tectonic and geomorphic stability of cratonic interiors: Earth and Planetary Science Letters, v. 219, p. 21-34.

Bierman, P.R., and Caffee, M., 2002, Cosmogenic exposure and erosion history of ancient Australian bedrock landforms: Geological Society of America Bulletin, v. 114, p. 787-803.

Bierman, P.R., and Caffee, M.W., 2001, Slow rates of rock surface erosion and sediment production across the Namib Desert and escarpment, Southern Africa: American Journal of Science, v. 301, p. 326-358.

Brown, E.T., Stallard, R.F., Larsen, M.C., Raisbeck, G.M., and Yiou, F., 1995, Denudation rates determined from the accumulation of in situ-produced ^{10}Be in the Luquillo Experimental Forest, Puerto Rico: Earth and Planetary Science Letters, v. 129, p. 193-202.

Clapp, E., Bierman, P.R., and Caffee, M., 2002, Using ^{10}Be and ^{26}Al to determine sediment generation rates and identify sediment source areas in an arid region drainage basin: Geomorphology, v. 45, p. 89-104.

Clapp, E.M., Bierman, P.R., Nichols, K.K., Pavich, M., and Caffee, M., 2001, Rates of sediment supply to arroyos from upland erosion determined using in situ produced cosmogenic ^{10}Be and ^{26}Al: Quaternary Research (New York), v. 55, p. 235-245.

Clapp, E.M., Bierman, P.R., Schick, A.P., Lekach, J., Enzel, Y., and Caffee, M., 2000, Sediment yield exceeds sediment production in arid region drainage basins: Geology, v. 28, p. 995-998.

Cockburn, H.A.P., Brown, R.W., Summerfield, M.A., and Seidl, M.A., 2000, Quantifying passive margin denudation and landscape development using a combined fission-track thermochronology and cosmogenic isotope analysis approach: Earth and Planetary Science Letters, v. 179, p. 429-435.

Duxbury, J., 2009, Erosion rates in and around Shenandoah National Park, VA, determined using analysis of cosmogenic ^{10}Be: Burlington, VT, University of Vermont.

Giardini, D., Grunthal, G., Shedlock, K.M., and Zhang, P., 1999, The GSHAP Global Seismic Hazard Map: ANNALI DI GEOFISICA, v. 42, p. 1225-1230.

Granger, D.E., Riebe, C.S., Kirchner, J.W., and Finkel, R.C., 2001, Modulation of erosion on steep granitic slopes by boulder armoring, as revealed by cosmogenic ^{26}Al and ^{10}Be: Earth and Planetary Science Letters, v. 186, p. 269-281.

Hancock, G., and Kirwan, M., 2007, Summit erosion rates deduced from 10Be: Implications for relief production in the central Appalachians: Geology, v. 35, p. 89-92.

Heimsath, A., Chappel, J., Finkel, R.C., Fifield, K., and Alimanovic, A., 2006, Escarpment Erosion and Landscape Evolution in Southeastern Australia: SPECIAL PAPERS-GEOLOGICAL SOCIETY OF AMERICA, v. 398, p. 173.

Heimsath, A.M., Chappell, J., Dietrich, W.E., Nishiizumi, K., and Finkel, R.C., 2000, Soil production on a retreating escarpment in southeastern Australia: Geology, v. 28, p. 787-790.

—, 2001a, Late Quaternary erosion in southeastern Australia: a field example using cosmogenic nuclides: Quaternary International, v. 83-85, p. 169-185.

Heimsath, A.M., Dietrich, W.E., Nishiizumi, K., and Finkel, R.C., 1997, The soil production function and landscape equilibrium: Nature (London), v. 388, p. 358-361.

—, 2001b, Stochastic processes of soil production and transport; erosion rates, topographic variation and cosmogenic nuclides in the Oregon Coast Range: Earth Surface Processes and Landforms, v. 26, p. 531-552.

Hijmans, R.J., Cameron, S.E., Parra, J.L., Jones, P.G., and Jarvis, A., 2005, Very high resolution interpolated climate surfaces for global land areas: International Journal of Climatology, v. 25, p. 1965-1978.

Ivy-Ochs, S., Kober, F., Alfimov, V., Kubik, F.W., and Synal, H.-A., 2007, Cosmogenic ^{10}Be, ^{21}Ne and ^{36}Cl in sanidine and quartz from Chilean ignimbrites: Nuclear Instruments and Methods in Physics Research, v. B, p. 6.

Jungers, M.C., 2008, Using 10-Be to determine sediment production and stransport rates on steep hillslopes in varied tectonic and climatic settings: Burlington, VT, University of Vermont.

Kober, F., Ivy-Ochs, S., Schlunegger, F., Baur, H., Kubik, P.W., and Wieler, R., 2007, Denudation rates and a topography-driven rainfall threshold in northern Chile: Multiple cosmogenic nuclide data and sediment yield budgets: Geomorphology, v. 83, p. 23.

Lal, D., 1991, Cosmic ray labeling of erosion surfaces; in situ nuclide production rates and erosion models: Earth and Planetary Science Letters, v. 104, p. 424-439.

Matmon, A.S., Bierman, P., Larsen, J., Southworth, S., Pavich, M., Finkel, R., and Caffee, M., 2003, Erosion of an ancient mountain range, the Great Smoky Mountains, North Carolina and Tennessee: American Journal of Science, v. 303, p. 817-855.

Nichols, K.K., Bierman, P.R., Foniri, W.R., Gillespie, A.R., Caffee, M., and Finkel, R., 2006, Dates and rates of arid region geomorphic processes: GSA Today, v. 16, p. 4-11.

Nishiizumi, K., Kohl, C.P., Arnold, J.R., Klein, J., Fink, D., and Middleton, R., 1991, Cosmic ray produced ^{10}Be and ^{26}Al in Antarctic rocks; exposure and erosion history: Earth and Planetary Science Letters, v. 104, p. 440-454.

Nishiizumi, K., Lal, D., Klein, J., Middleton, R., and Arnold, J.R., 1986, Production of ^{10}Be and ^{26}Al by cosmic rays in terrestrial quartz in situ and implications for erosion rates: Nature, v. 319, p. 134-136.

Peel, M.C., Finlayson, B.L., and McMahon, T.A., 2007, Updated world map of the Koppen-Geiger climate classification: Hydrology and Earth System Sciences, v. 11, p. 1633-1644.

Quigley, M., Sandiford, M., Fifield, K., and Alimanovic, A., 2007, Bedrock erosion and relief production in the northern Flinders Ranges, Australia: Earth Surface Processes and Landforms, v. 32, p. 929.

Reinhardt, L.J., Bishop, P., Hoey, T.B., Dempster, T.J., and Sanderson, D.C.W., 2007, Quantification of the transient response to base-level fall in a small mountain catchment: Sierra Nevada, southern Spain: Journal of Geophysical Research, v. 112.

Reuter, J.M., 2005, Erosion rates and patterns inferred from cosmogenic ^{10}Be in the Susquehanna River basin: Burlington, VT, University of Vermont.

Saunders, I., and Young, A., 1983, Rates of surface processes on slopes, slope retreat, and denudation: Earth Surface Processes and Landforms, v. 8, p. 473-501.

Small, E.E., Anderson, R.S., Repka, J.L., and Finkel, R., 1997, Erosion rates of alpine bedrock summit surfaces deduced from in situ ^{10}Be and ^{26}Al: Earth and Planetary Science Letters, v. 150, p. 413-425.

Sullivan, C.L., 2007, ^{10}Be erosion rates and landscape evolution of the Blue Ridge Escarpment, southern Appalachian Mountains: Burlington, VT, University of Vermont.

Trodick, C., In Progress, Sediment Generation Rates on the Potomac River Basin Burlington, VT, University of Vermont.

Vance, D., Bickle, M., Ivy-Ochs, S., and Kubik, P.W., 2003, Erosion and exhumation in the Himalaya from cosmogenic isotope inventories of river sediments: Earth and Planetary Science Letters, v. 206, p. 273-288.

von Blanckenburg, F., Hewawasam, T., and Kubik, P.W., 2004, Cosmogenic nuclide evidence for low weathering and denudation in the wet, tropical highlands of Sri Lanka: Journal of Geophysical Research, v. 109.

Ward, I.A.K., Nanson, G.C., Head, L.M., Fullagar, R.L.K., Price, D.M., and Fink, D., 2005, Late Quaternary landscape evolution in the Keep River region, northwestern Australia: Quaternary Science Reviews, v. 24, p. 1906-1922.

Weissel, J.K., and Seidl, M.A., 1998, Inland propagation of erosional escarpments and river profile evolution across the southeast Australian passive continental margin: Geophysical Monograph, v. 107, p. 189-206.

7.0 Figures and Tables
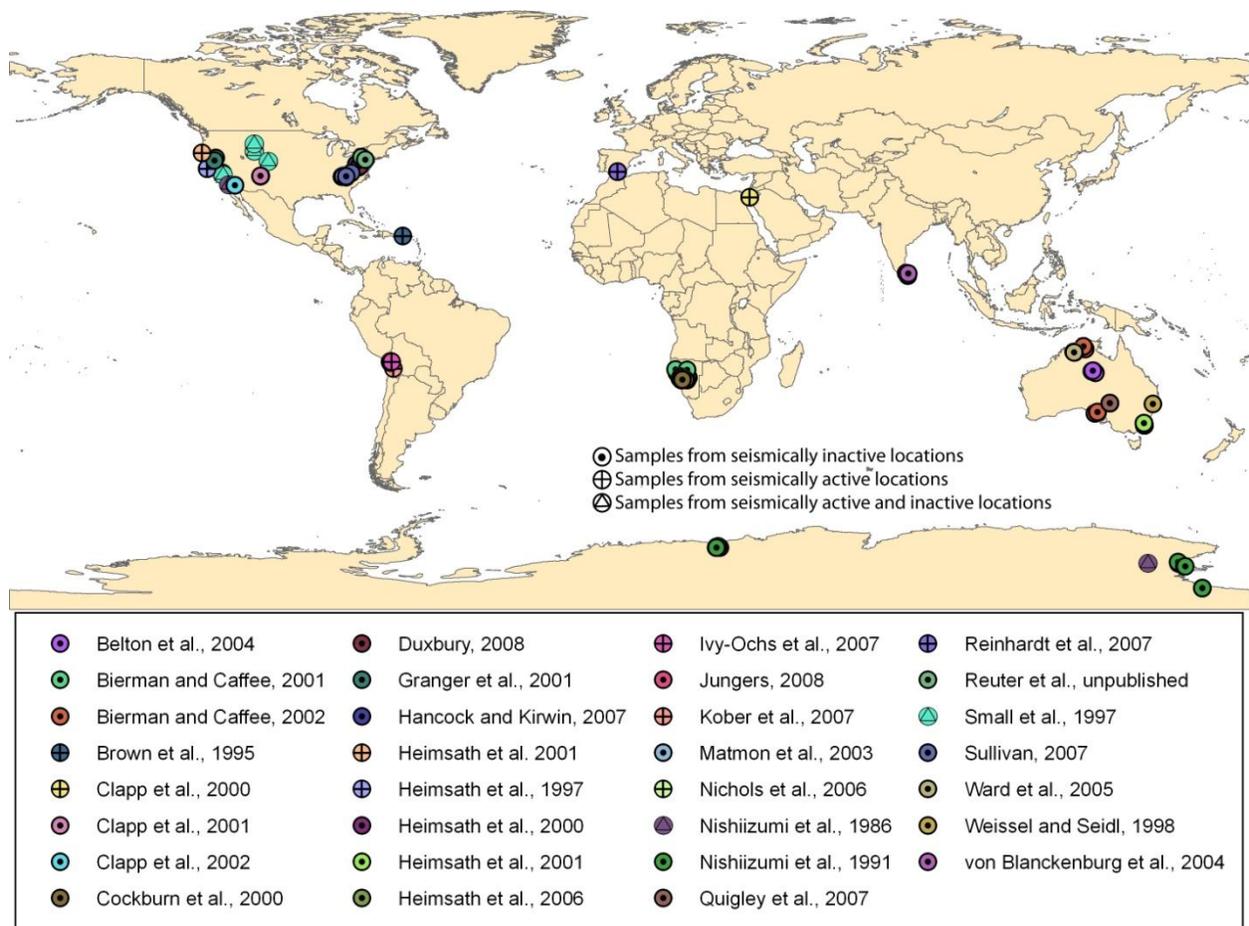
Figure 1. Studies from which bedrock erosion rate data were collected (Belton et al., 2004; Bierman and Caffee, 2002; Bierman and Caffee, 2001; Brown et al., 1995; Clapp et al., 2002; Clapp et al., 2001; Clapp et al., 2000; Cockburn et al., 2000; Duxbury, 2009; Granger et al., 2001; Hancock and Kirwan, 2007; Heimsath et al., 2006; Heimsath et al., 2000, 2001a; Heimsath et al., 1997, 2001b; Ivy-Ochs et al., 2007; Jungers, 2008; Matmon et al., 2003; Nichols et al., 2006; Nishiizumi et al., 1991; Nishiizumi et al., 1986; Quigley et al., 2007; Reinhardt et al., 2007; Reuter, 2005; Small et al., 1997; Sullivan, 2007; von Blanckenburg et al., 2004; Ward et al., 2005; Weissel and Seidl, 1998). Seismic activity for each study location was determined using the output from the Global Seismic Hazard Assessment Program (Giardini et al., 1999).
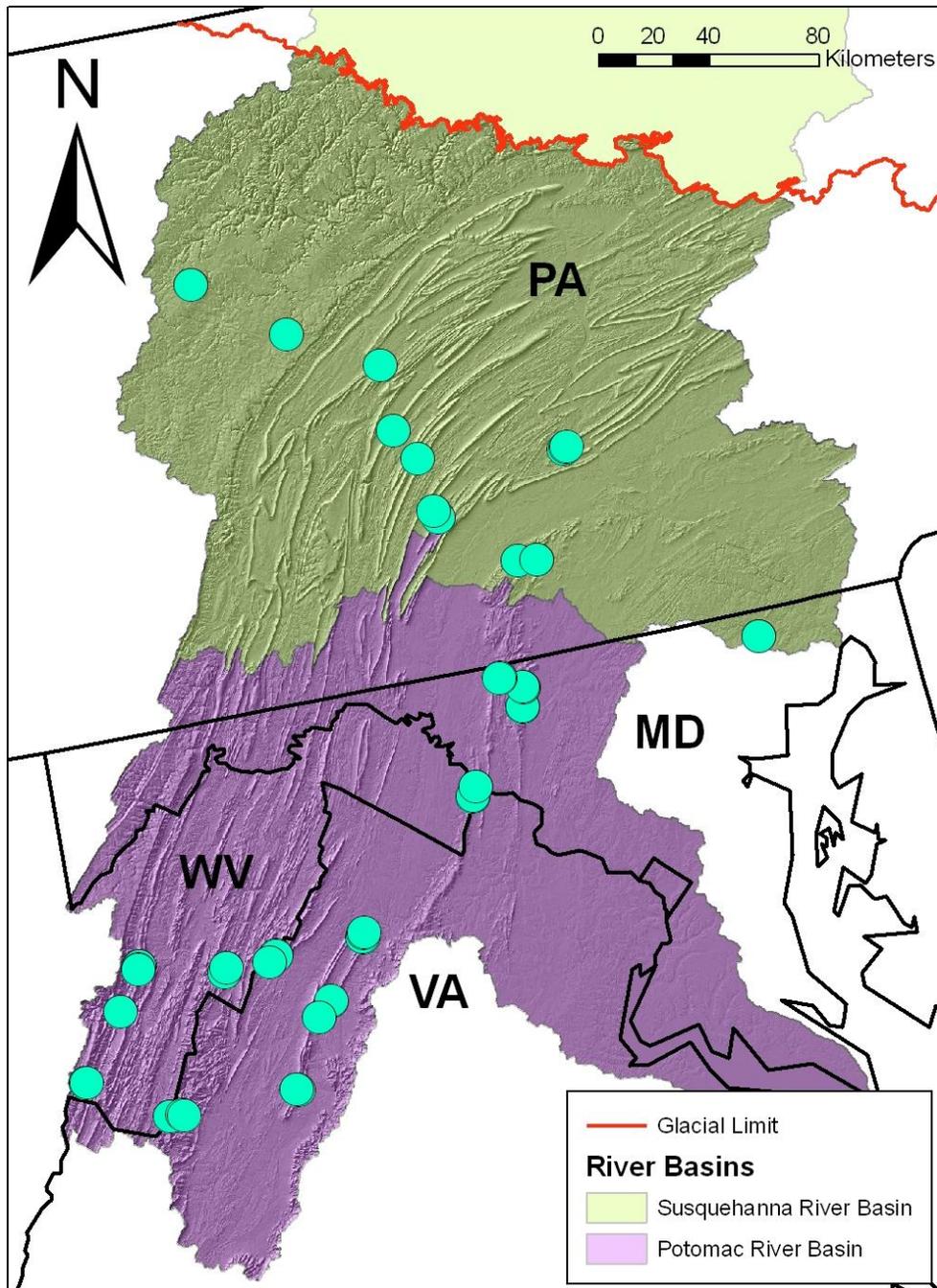
Figure 2. Field sites where bedrock samples were collected in the Summer of 2009.
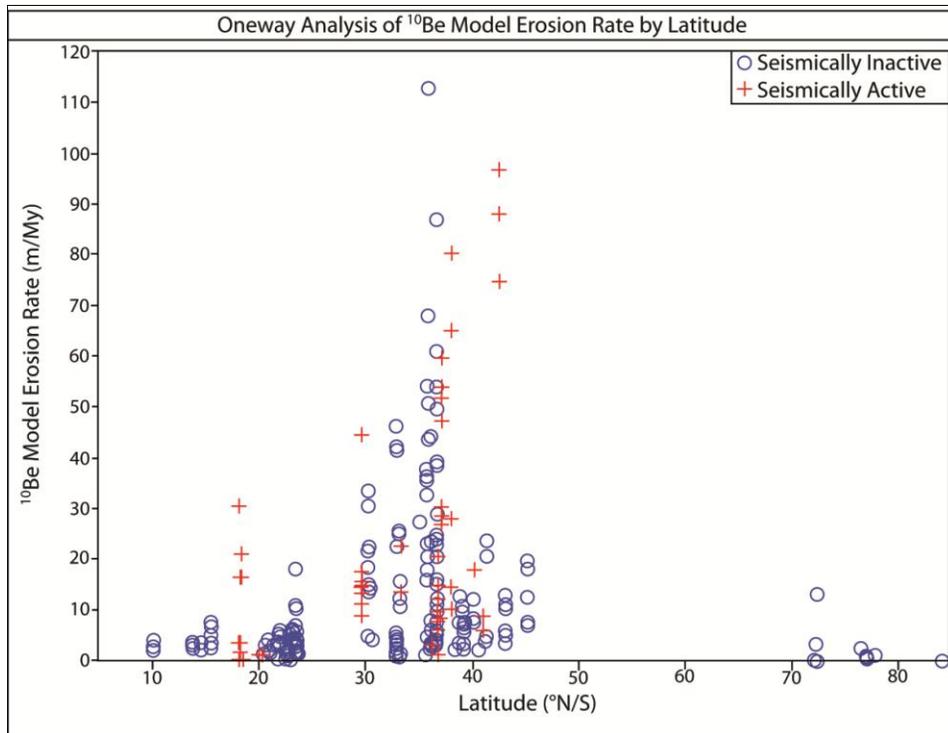
Figure 3. Global erosion rates plotted against latitude. Sampling gaps are seen between 50°-70°. Erosion rates are highest at latitudes where most temperate and cold climate zones are situated.
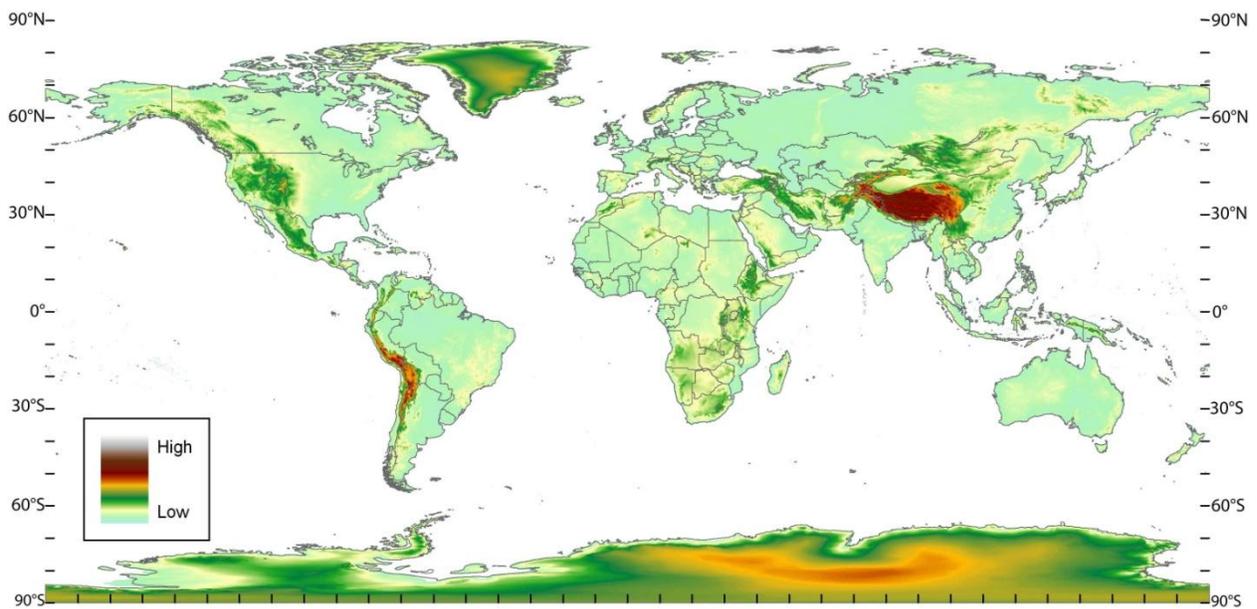
Figure 4. GTopo_30 elevation dataset used for elevation and local relief analyses. Resolution is 30 arc seconds or ~1km.
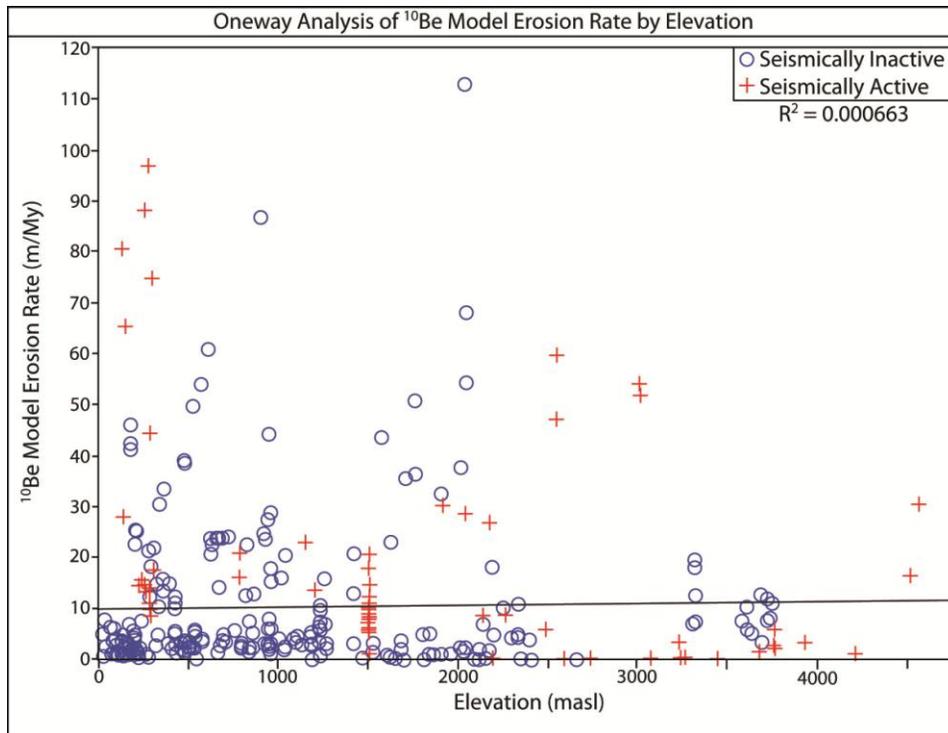
Figure 5. Elevation (in meters above sea level) yielded the weakest fit of any regression.
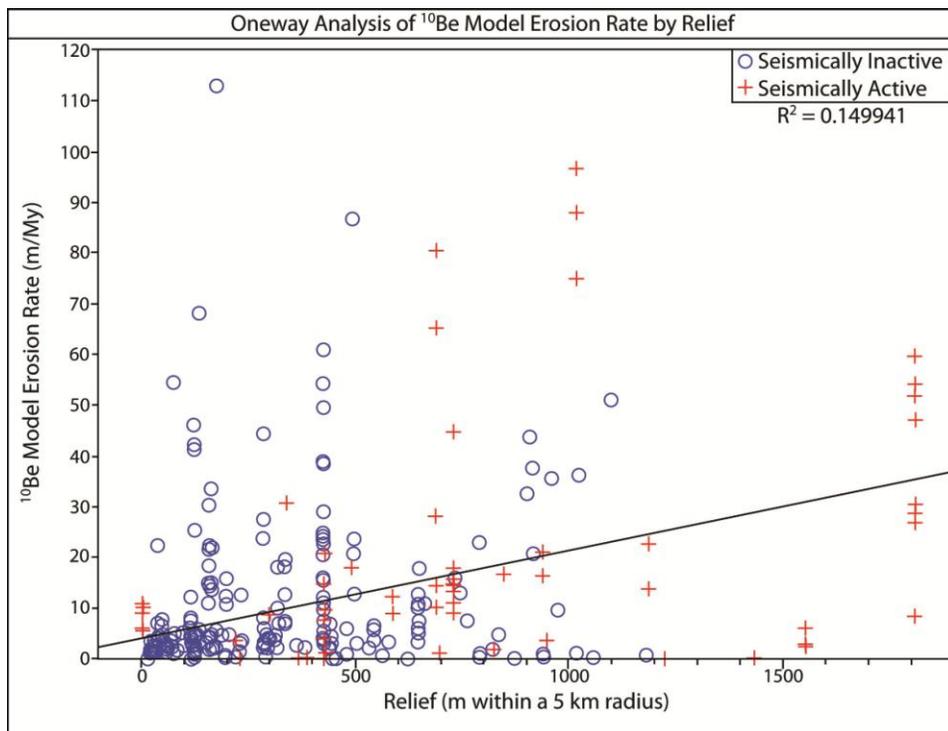
Figure 6. Erosion rates plotted against local relief yielded one of the strongest regression of any variable tested.
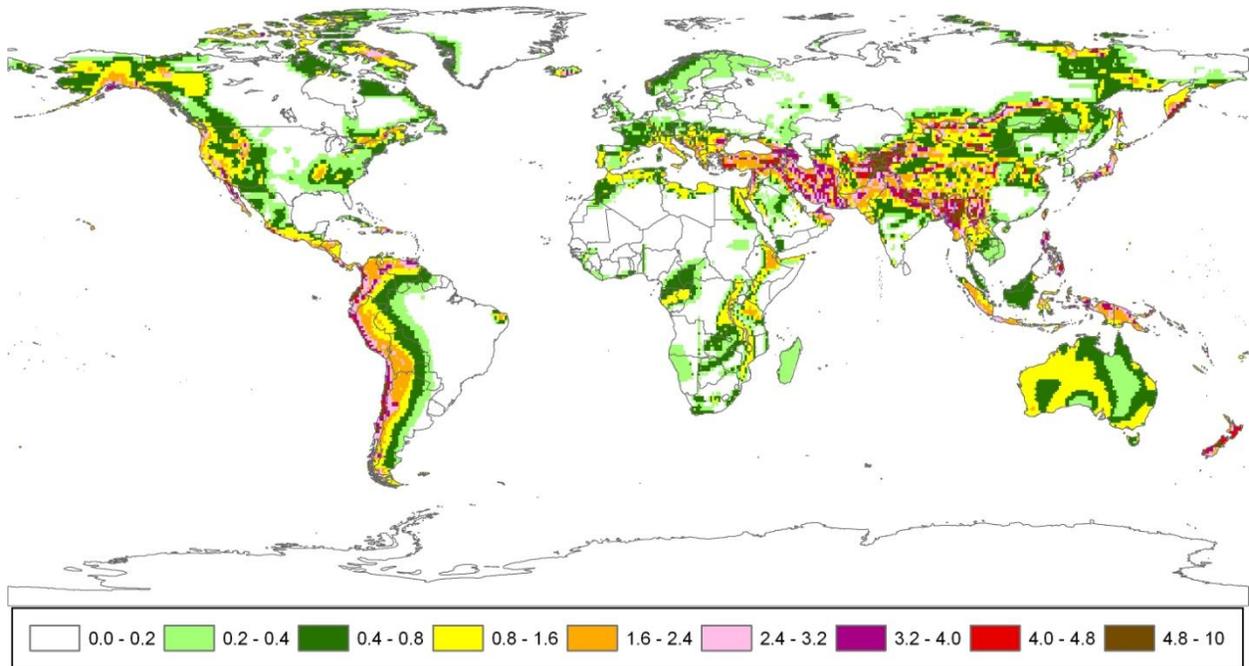
Figure 7. Global Seismic Hazard Map produced by Giardini et al. (1999). This map is the basis for seismic zone delineation seen in Figs. 1 and 9. Study sites in green or white were deemed seismically inactive unless the publication presented strong evidence otherwise.
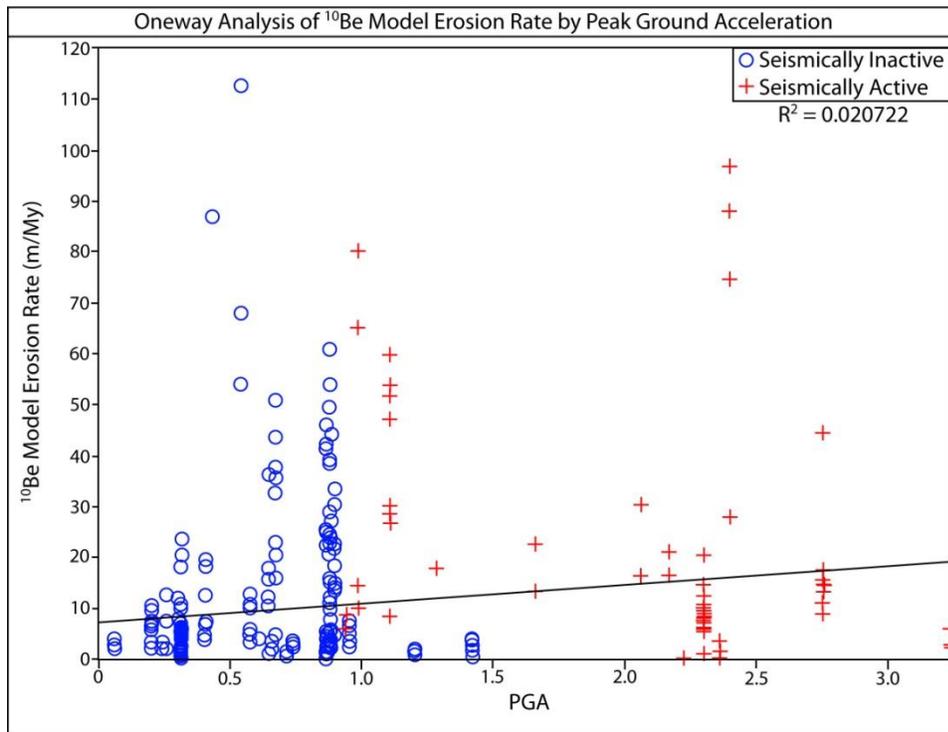
Figure 8. Though basin-averaged erosion rates correlate to peak ground acceleration (Reuter, 2005), only a weak correlation is seen with bedrock erosion rates.
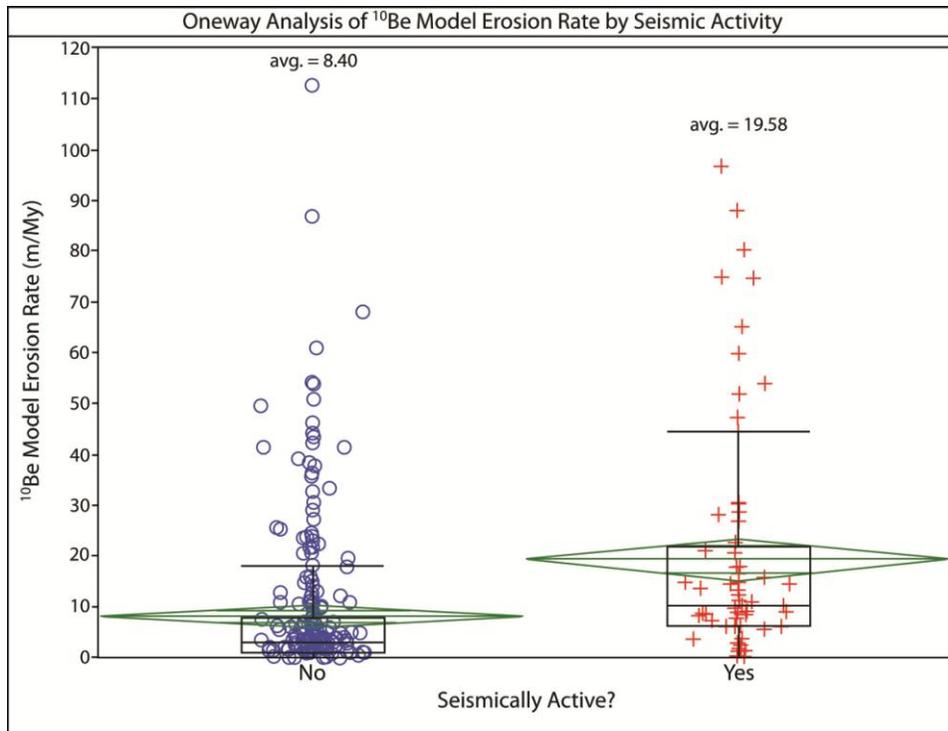
Figure 9. Erosion rates in seismically active regions are significantly higher than those in inactive regions.
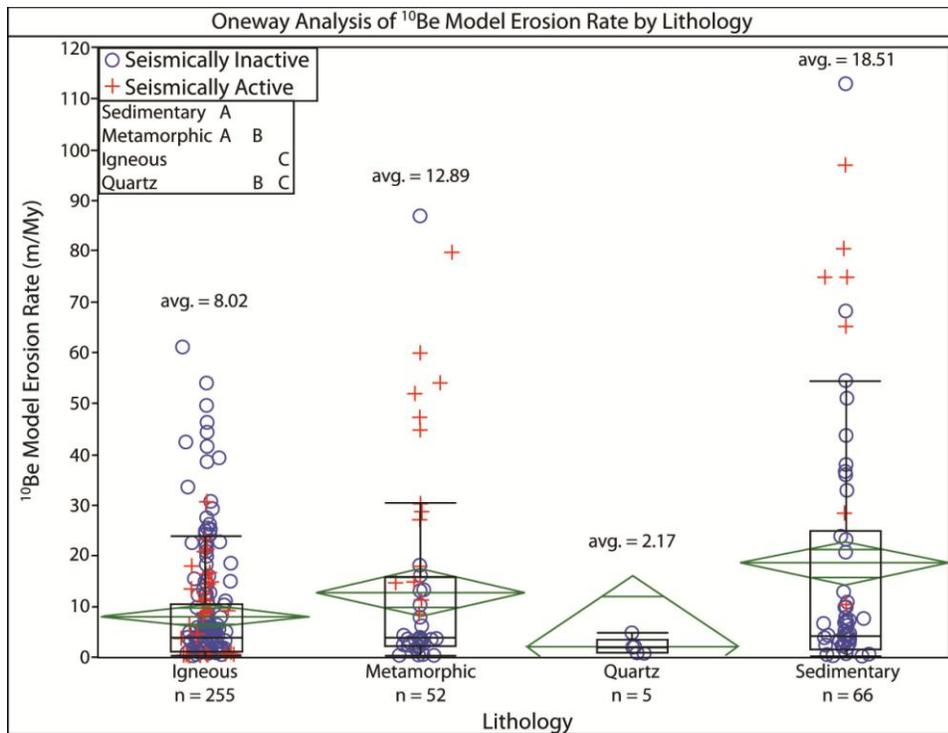
Figure 10. Erosion rates plotted against lithology. Lithologies not connected by a common letter in the subset figure are significantly different.
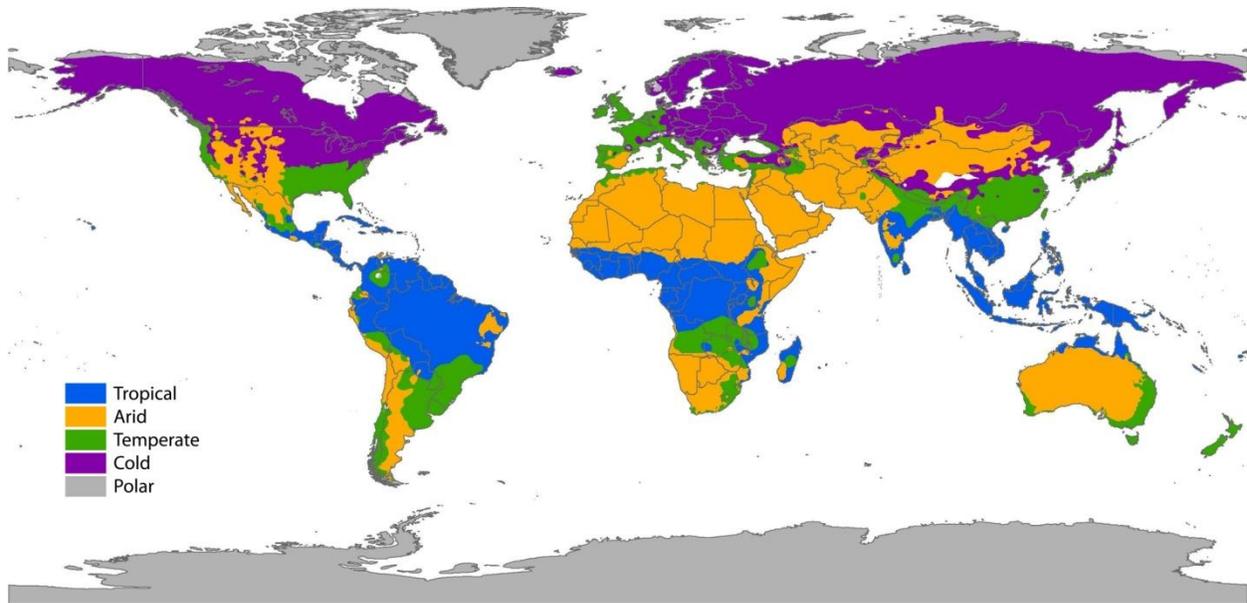
Figure 11. Köppen-Geiger climate zone map after Peel et al. (2007).
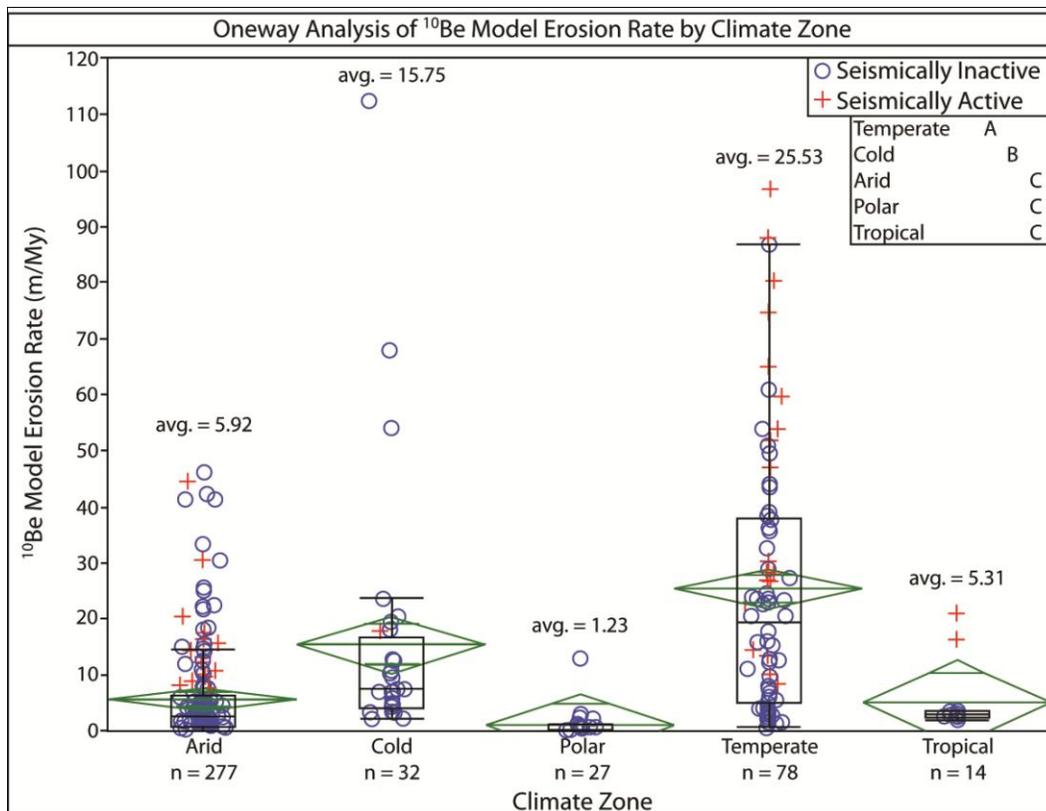
Figure 12. Erosion rates plotted again Köppen-Geiger climate zone classes. Climate zones not connected by a common letter in the subset figure are significantly different.
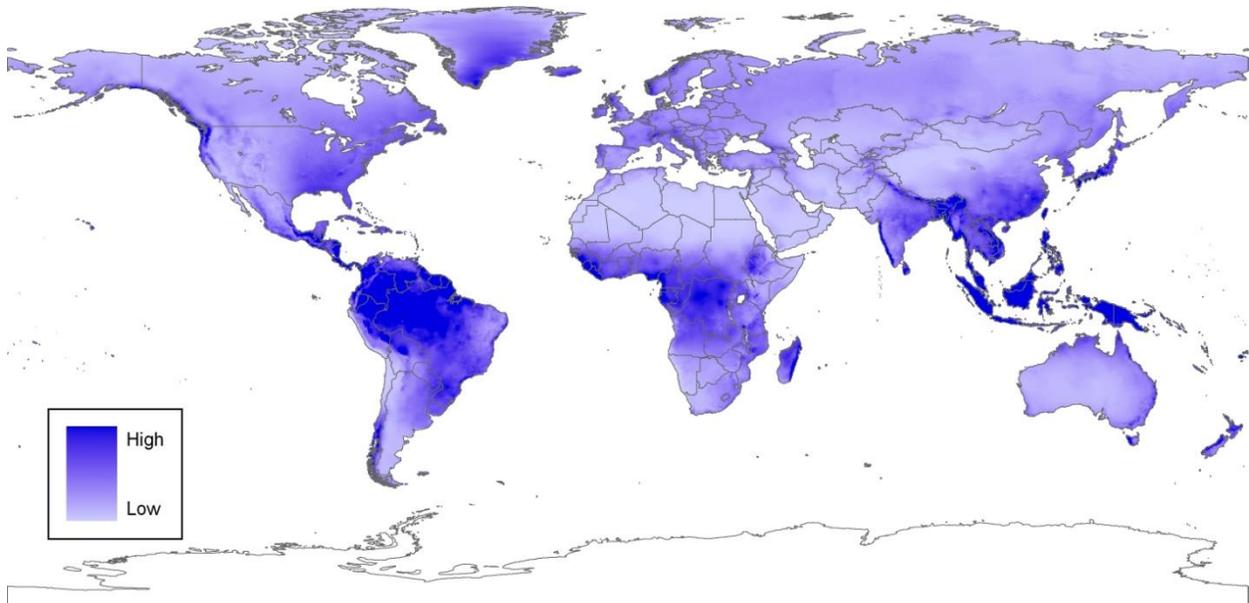
Figure 13. Mean annual precipitation in mm/yr (Hijmans et al., 2005).
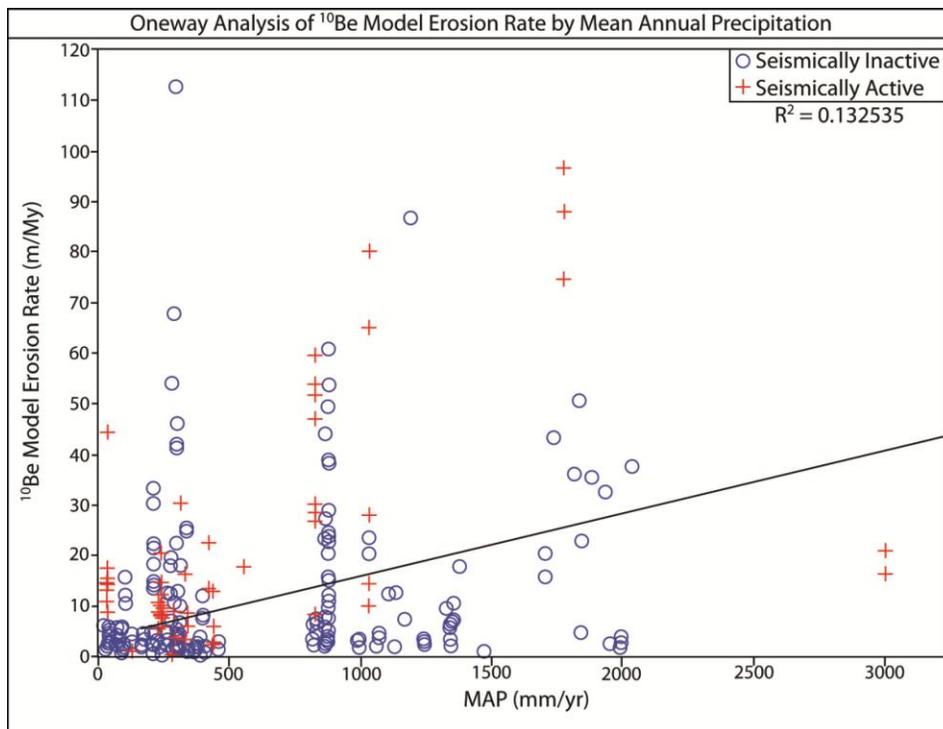
Figure 14. Mean annual precipitation yields one of the strongest regressions with erosion rates on the global scale.
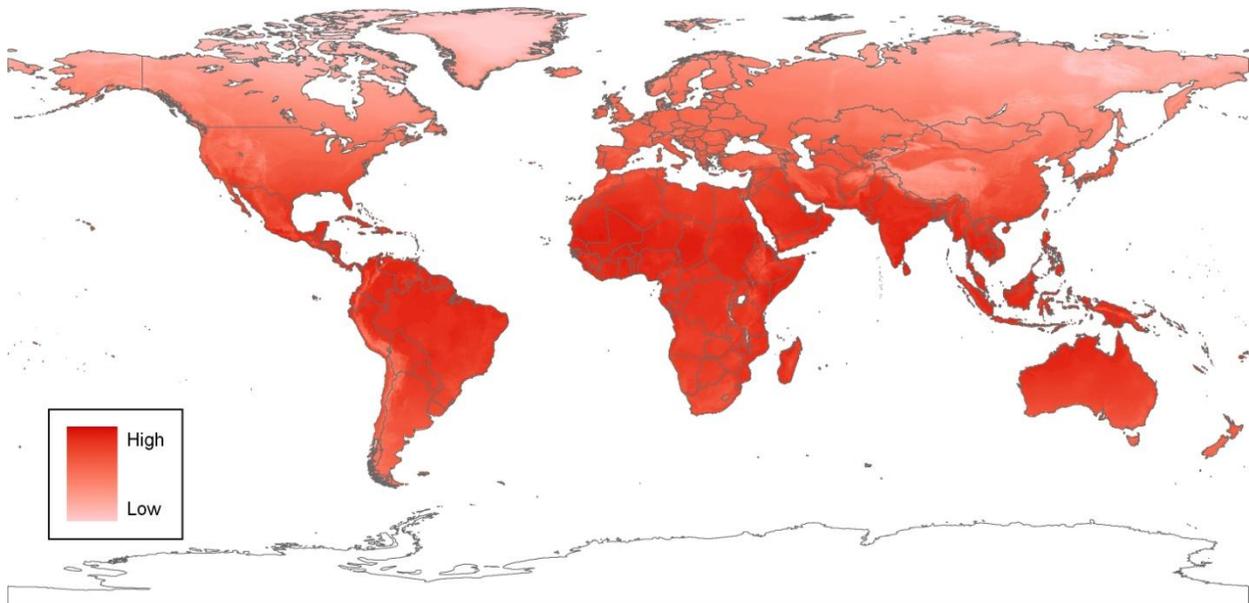
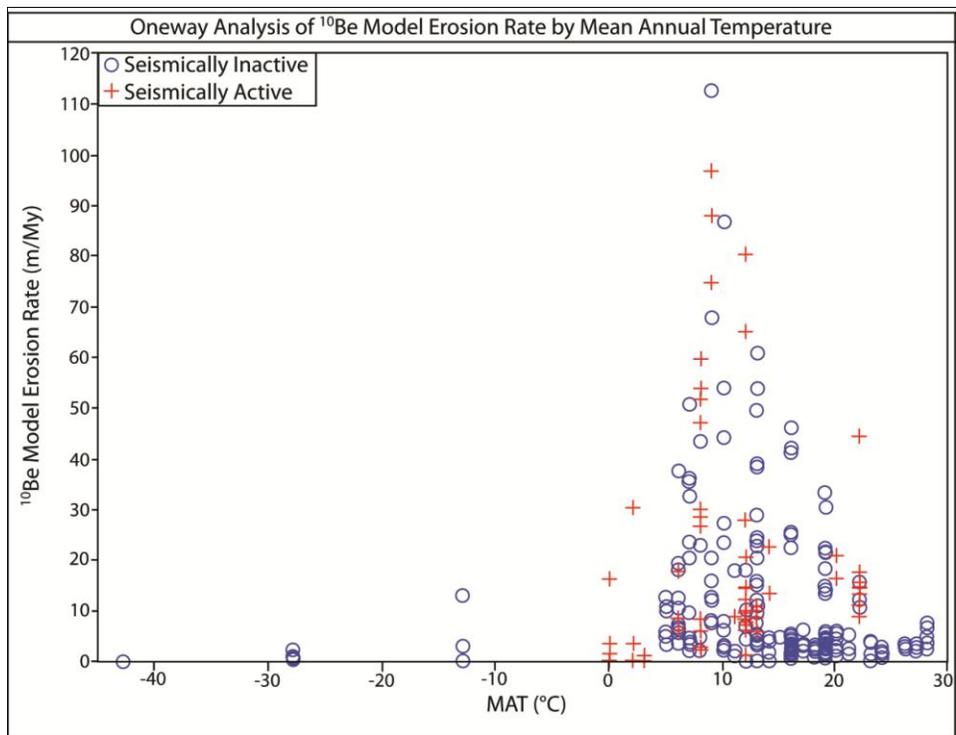Figure 15. Mean annual temperature (°C; Hijmans et al., 2005).

Figure 12. A quadratic regression best fits the mean annual temperature data as low erosion rates are seen at both very high and low temperatures.

Figure 17. Forward stepwise regression summary table. Regressions were run for each of the categories along the top. The number of samples in each category is provided by n. Variables used in each regression are listed along the left. Boxes with a black circle indicate the variables which are significantly significant for each category. The number in the black circle indicates the level of importance assigned to the variable (1=most important). The percentage of variance described by the regression is given by R^2.

Table 1. Global datasets used to extract parameter values for each point.

Variable	Dataset
Elevation	Gtopo_30: provided by ESRI Software at University of Vermont
Local Relief	Same as Elevation
Peak Ground Acceleration	Global Seismic Hazard Assessment Program (Giardini et al., 1999)*
Climate Zone	Köppen-Geiger Climate System (Peel et al., 2007)
Mean Annual Precipitation	WorldClim Climate Model (Hijmans et al., 2005) †
Mean Annual Temperature	Same as Mean Annual Precipitation†

*Dataset does not cover Antarctica. Antarctic sites were not used in bivariate analysis or forward stepwise regression.

†Dataset did not cover Antarctica. Data for sites in Antarctica were provided by the Hindcast model provided by the Polar Meteorology Group at Ohio State University (http://polarmet.mps.ohio-state.edu/).

Table 2. Timeline of the completion of my research and degree work.

December 2009	- Finish bedrock and basin-averaged data compilation and begin writing manuscript - Continue quartz purity tests - Begin *in situ* laboratory methods
January 2010	- Finish *in situ* laboratory work - Submit global summary manuscript (journal TBA)
March 2010	- Run samples using AMS at Lawrence Livermore National Laboratory - Receive data
April 2010	Data Analysis
Summer 2010	- Write thesis - Write manuscript for Appalachian bedrock paper
Fall 2010	- Defend thesis in early Fall - Prepare for/give talk at GSA